

Research Article

Adjusting the stiffness of a cell-free hydrogel system based on tissue-specific extracellular matrix to optimize adipose tissue regeneration

Ye Li^{1,†}, Xin Bi^{1,2,†}, Mengfan Wu¹, Xinyao Chen¹, Weiqing Zhan³, Ziqing Dong^{1,*} and Feng Lu^{1,*}

¹Department of Plastic and Cosmetic Surgery, Nanfang Hospital, Southern Medical University, 1838 Guangzhou North Road, Guangzhou, Guangdong 510515, P. R. China; ²Dermatology Department, The First People's Hospital of Yunnan Province, 157 Jinbi Road, Xishan district, Kunming, Yunnan province 650100, P. R. China; and ³Department of Plastic and Cosmetic Surgery, Third Affiliated Hospital of Southern Medical University, 139 Zhongshan Avenue West, Guangzhou, Guangdong 510515, P.R. China

*Correspondence. Feng Lu, Email: doctorlufeng@hotmail.com; Ziqing Dong, Email: doctordongziqing@hotmail.com

[†]These authors contributed equally to this work and are co-first authors.

Received 29 June 2022; Revised 26 August 2023; Editorial decision 12 January 2023

Abstract

Background: Large-area soft tissue defects are challenging to reconstruct. Clinical treatment methods are hampered by problems associated with injury to the donor site and the requirement for multiple surgical procedures. Although the advent of decellularized adipose tissue (DAT) offers a new solution to these problems, optimal tissue regeneration efficiency cannot be achieved because the stiffness of DAT cannot be altered *in vivo* by adjusting its concentration. This study aimed to improve the efficiency of adipose regeneration by physically altering the stiffness of DAT to better repair large-volume soft tissue defects.

Methods: In this study, we formed three different cell-free hydrogel systems by physically cross-linking DAT with different concentrations of methyl cellulose (MC; 0.05, 0.075 and 0.10 g/ml). The stiffness of the cell-free hydrogel system could be regulated by altering the concentration of MC, and all three cell-free hydrogel systems were injectable and moldable. Subsequently, the cell-free hydrogel systems were grafted on the backs of nude mice. Histological, immunofluorescence and gene expression analyses of adipogenesis of the grafts were performed on days 3, 7, 10, 14, 21 and 30.

Results: The migration of adipose-derived stem cells (ASCs) and vascularization were higher in the 0.10 g/ml group than in the 0.05 and 0.075 g/ml groups on days 7, 14 and 30. Notably, on days 7, 14 and 30, the adipogenesis of ASCs and adipose regeneration were significantly higher in the 0.075 g/ml group than in the 0.05 g/ml group ($p < 0.01$ or $p < 0.001$) and 0.10 g/ml group ($p < 0.05$ or $p < 0.001$).

Conclusion: Adjusting the stiffness of DAT via physical cross-linking with MC can effectively promote adipose regeneration, which is of great significance to the development of methods for the effective repair and reconstruction of large-volume soft tissue defects.

Key words: Stiffness, Extracellular matrix, Adipose tissue, Regeneration, Adipose-derived stem cells, Hydrogel, Stiffness

Highlights

- A novel cell-free hydrogel system with varying degrees of stiffness was designed and constructed.
- Increasing the stiffness of the cell-free hydrogel system promoted the migration of ASCs and vascularization after grafting.
- Adipose regeneration was highest in the cell-free hydrogel system with suitable stiffness.

Background

Large-area soft tissue defects caused by trauma or medical treatments are difficult to reconstruct through surgery. At present, autologous skin flaps, fat grafts or other fillers are typically used to reconstruct such defects [1–5]. However, these treatments are hampered by a risk of injury to the donor site and the requirement for multiple surgical procedures. Recently, the use of decellularized adipose tissue (DAT) has provided a new solution to the problem [6,7]. A substantial quantity of human extracellular matrix (ECM), including basement membrane components, can be isolated from DAT, a tissue source that is widely available and commonly discarded [8,9]. Methods have now been developed to extract intact ECM scaffolds with well-preserved 3D structures, suitable for large-volume augmentation [10].

DAT was first described as a scaffold for adipose tissue regeneration by Flynn in 2010 [11]. In a more recent 16-week study, injection of DAT into the human dorsal wrist successfully promoted adipose tissue regeneration [12]. Both of these studies reported high expression levels of adipogenic markers in the scaffolds and the promotion of adipogenesis by DAT. Notably, the DAT microenvironment was sufficient to induce the expression of peroxisome proliferator-activated receptor gamma (PPAR γ) and transcription factor CCAAT/enhancer-binding protein alpha (C/EBP α), the master regulators of adipogenesis, without the need for exogenous differentiation factors [11]. The successful use of DAT scaffolds for tissue regeneration highlights the importance of the cell donor source in the development of tissue-engineering strategies that incorporate adipose-derived stem cells (ASCs).

DAT can promote the migration of ASCs and ensure a sufficient supply of seed cells for regeneration *in vivo*. However, the ability of ordinary DAT to support adipogenic differentiation of ASCs is hindered by its excessive stiffness [13]. In previous *in vitro* studies, the concentration of DAT was altered to achieve a stiffness of 2–4 kPa, which is optimal for fat regeneration [14]. However, the optimal stiffness for DAT-induced ASC migration and adipogenic differentiation could not be determined because the concentration of DAT could not be adjusted in *in vivo* studies.

Here, to test the hypothesis that regulating the stiffness of DAT could improve the adipogenesis of ASCs and subsequent adipose regeneration, we physically cross-linked three different concentrations of methyl cellulose (MC) with the same volume of DAT to form cell-free hydrogel systems. Subsequently, we examined the effects of cross-linking with MC on the stiffness and microstructure of DAT, as well as on ASC migration and adipose regeneration after grafting, in comparison with grafting of DAT, which we explored previously.

Methods

Adipose tissue procurement

This study was approved by the Ethics Committee of the Southern Medical University, Nanfang Hospital, China. Lipoaspirate was obtained from 10 non-obese, healthy female human donors (information about the patients is provided in [supplementary Table 1](#), see online supplementary material) aged 20–45 years with a body mass index of 22.8 ± 2.7 kg/m² who underwent liposuction at Nanfang Hospital. Abdominal or femoral fat was harvested using the tumescent technique by infiltrating with saline (1:1,000,000 epinephrine), and subcutaneous fat was suctioned manually using a 20 cc syringe equipped with a 3.0 mm cannula. The samples were stored in sterile, cation-free phosphate-buffered saline supplemented with 20 mg/ml bovine serum albumin and were delivered to the laboratory on ice for processing within 2 h of extraction.

Adipose tissue decellularization and generation of cell-free hydrogel systems

The optimized decellularization protocol is shown in [Figure 1](#) and described in detail in [supplementary Table 2](#) (see online supplementary material). In brief, the detergent-free extraction procedure involved mechanical disruption, polar solvent extraction, enzymatic digestion, sterilization and mixing with MC to form a cell-free hydrogel system. Three different cell-free hydrogel systems were generated with different concentrations of MC (0.05, 0.075 and 0.10 g/ml).

Scanning electron microscopy

The cell-free hydrogel systems were fixed with 2% glutaraldehyde and then treated with 1% osmium tetroxide for 1 h. The samples were then dehydrated in acetone, sputtered with gold using a MED 010 coater, and examined under an S-3000 N scanning electron microscope (Hitachi, Ltd, Tokyo, Japan). Details of the operating protocol are provided in our previous studies [15,16].

Stiffness testing

A Bose ElectroForce[®] load-testing device (TA Instruments, New Castle, DE, USA) was used to measure stiffness, as described in our previous study [14]. Specifically, the load cell used to measure forces ranged from 0 to 225 N. The device's electromagnetic actuator permitted axial travel of 6 mm. Therefore, a preload was applied to remove slack from tissues and induce elongation. Each tissue sample was clamped and then a preload (25–30 N) was applied followed

Histological analysis

Samples were fixed in 4% paraformaldehyde, dehydrated, embedded in paraffin and then stained with hematoxylin–eosin and Masson's trichrome. The samples were sectioned and examined under a BX51 microscope (Olympus Corporation, Shibuya, Japan). Images were acquired using a DP71 digital camera (Olympus Corporation).

Immunofluorescence

For immunofluorescence staining, tissue samples were incubated with rat anti-CD31 (1:200; Abcam, Cambridge, MA, USA), rat anti-CD34 (1:200, Abcam) and rabbit anti-mouse perilipin (1:400; Progen, Heidelberg, Germany) antibodies. After washing, the samples were incubated with donkey anti-rat Alexa Fluor 555 IgG (Abcam) and goat anti-rabbit Alexa Fluor 430 IgG (Invitrogen, North Ryde, NSW, Australia) antibodies. Nuclei were stained with 4',6-diamidino-2-phenylindole (DAPI) (Sigma, St. Louis, MO, USA) [18,19].

Western blotting

Total cell lysates of the samples were prepared using M-PER Mammalian Protein Extraction Reagent (ThermoFisher Scientific, Waltham, MA, USA). A bicinchoninic acid (BCA) protein assay (ThermoFisher Scientific) was used to estimate the concentration of the protein. After separation by sodium dodecyl sulfate–polyacrylamide gel electrophoresis using a NuPAGE electrophoresis system, protein extracts were transferred to immobilized polyvinylidene difluoride membranes (Millipore, Billerica, MA, USA). The membranes were blocked in 5% milk and then incubated with the following primary antibodies: anti-PPAR- γ (1:200, Abcam), anti-C/EBP (1:1000, Abcam) and anti-adipocyte protein 2 (aP2; 1:1000, Abcam). Thereafter, the membranes were incubated with secondary antibodies and a WesternBreeze Chemiluminescent Detection Kit (ThermoFisher Scientific) was used to detect signals. Glyceraldehyde-3-phosphate dehydrogenase (GAPDH) served as an internal control.

Statistical analysis

Statistical analyses were performed using IBM SPSS version 22.0 (IBM Corp., Armonk, NY, USA). Data are expressed as the mean \pm SD. One-way analysis of variance and the Kruskal–Wallis test were used to compare the three groups at the same time point. Comparisons between two groups (0.05 vs. 0.075 g/ml, 0.075 vs. 0.10 g/ml and 0.05 vs. 0.10 g/ml) at single time points were performed using the independent Student's *t*-test; $p < 0.05$ was considered statistically significant.

Results

Grafting of DAT

DAT was injected into the backs of nude mice and observed on day 30 (supplementary Figure S1a, b). The surface of the graft was covered with multiple blood vessels and the graft

felt slightly hard. Hematoxylin–eosin and Masson's trichrome staining of the grafts showed that there were few mature adipocytes, which were mainly concentrated at the edge of the grafts (supplementary Figure S1c, d). Immunofluorescence staining revealed that although some CD31-positive areas were present in the graft, there were only a few perilipin-positive cells, which were mainly concentrated at the edge of the grafts (supplementary Figure S1e).

Stiffness of the cell-free hydrogel system

Three cell-free hydrogel systems were generated by cross-linking DAT with an equal volume of different concentrations of MC (0.05, 0.075 or 0.10 g/ml). All three cell-free hydrogel systems were injectable and moldable (Figure 2a). The stiffness of DAT was significantly attenuated by cross-linking with MC (supplementary Figure S2a, see online supplementary material). In addition, the concentration of MC was proportional to the stiffness of the sample and there were significant differences in stiffness and rheological properties between the three groups (Figure 2b and supplementary Figure S2b).

Microstructure of the cell-free hydrogel system

Scanning electron microscopy analyses showed that DAT and MC were fully cross-linked in all three groups. The microstructure of the 0.05 g/ml group was the least dense and that of the 0.10 g/ml group was the densest (Figure 2c). The concentration of MC was proportional to the porosity of the sample: the porosity of the 0.05 g/ml group was significantly higher than those of the 0.075 g/ml ($p < 0.05$) and 0.10 g/ml ($p < 0.01$) groups (Figure 2d). This indicates that the retention rate of grafts was highest at a stiffness of 4 kPa.

Sample volume and oil red O staining of grafts

Next, the three cell-free hydrogel systems were injected into the backs of nude mice (Figure 3a). The appearance of the grafts in the three groups did not differ; however, the grafts in the 0.05 g/ml group were soft, whereas those in the 0.10 g/ml group were hard. The tactile feel of the grafts in the 0.075 g/ml group was similar to that of adipose tissue (Figure 3b). In all groups, the volumes of the cell-free hydrogel samples decreased after grafting into mice. However, the percent volume retention of the grafts in the 0.075 g/ml group was higher than that of the grafts in the 0.05 and 0.10 g/ml groups on day 30 ($p < 0.05$) (Figure 3d). Oil red O staining of grafts on day 30 showed that the lipid area in the 0.075 g/ml group was higher than that in the 0.05 and 0.10 g/ml groups, and that in the 0.05 g/ml group was the lowest (Figure 3c). This indicates that the adipogenesis of grafts was highest at a stiffness of 4 kPa.

Vascularization of grafts

Immunofluorescence staining showed that more CD31-positive areas were present in grafts in the 0.10 g/ml group

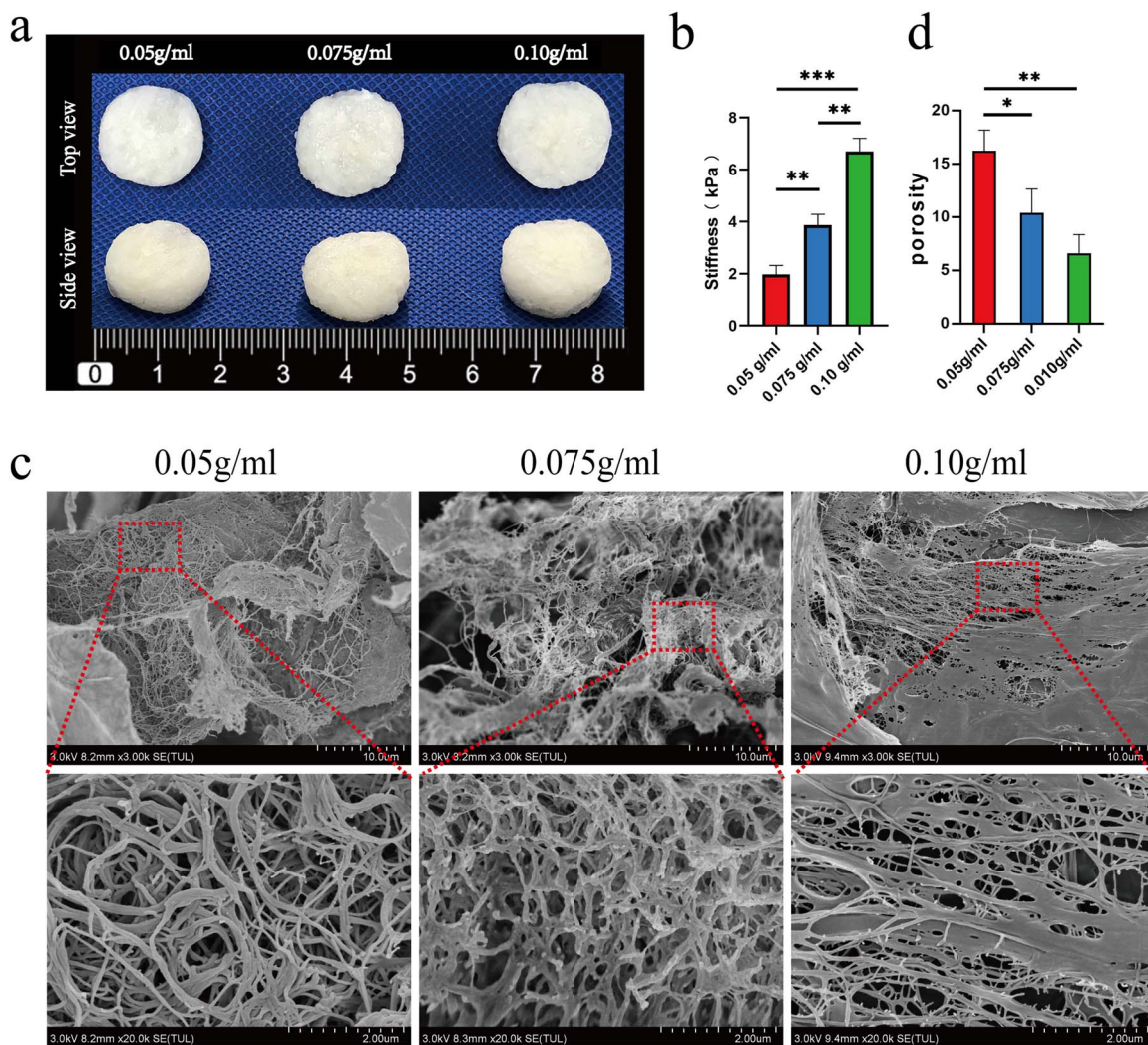


Figure 2. Gross morphologies, stiffnesses and microstructures of the cell-free hydrogel systems. (a) Top and side views of each cell-free hydrogel system, showing the concentrations of MC used for cross-linking. (b) Stiffness analysis of the three cell-free hydrogel systems. (c) Scanning electron microscopy images of the three cell-free hydrogel systems. The red boxes are magnified in the lower images. (d) Porosity analysis of the cell-free hydrogel systems (* $p < 0.05$, ** $p < 0.01$, *** $p < 0.001$; $n = 7$). Scale bar: 10 or 2 μm

than in grafts in the 0.05 and 0.075 g/ml groups on day 30 (Figure 3c). The number of capillaries per optical field in the 0.05 g/ml group was significantly lower than that in the 0.075 g/ml group ($p < 0.001$ or $p < 0.01$) and 0.10 g/ml group (all $p < 0.001$) on days 7 and 14. In addition, the number of capillaries per optical field in the 0.10 g/ml group was significantly higher than that in the 0.05 g/ml group ($p < 0.001$) and 0.075 g/ml group ($p < 0.01$) on day 30 (Figure 3e). This indicates that the higher the stiffness of the graft, the greater the level of neovascularization in the graft.

Histologic evaluation of grafts

Hematoxylin–eosin and Masson’s trichrome staining of the grafts on days 7, 14 and 30 after injection into nude mice showed that the density of cells observed per unit area of the grafts was proportional to the concentration of MC used for cross-linking (Figure 4a, b). In addition, more cells

were observed in the 0.075 and 0.10 g/ml groups than in the 0.05 g/ml group (Figure 4a). The percentage of collagen, which was determined based on Masson’s staining, was lower in the 0.05 g/ml group than in the 0.075 and 0.10 g/ml groups on days 7 ($p < 0.001$), 14 ($p < 0.05$) and 30 ($p < 0.001$). In addition, the percentage of collagen was higher in the 0.10 g/ml group than in the 0.075 g/ml group on days 7 ($p < 0.05$) and 30 ($p < 0.01$) (Figure 4c). This suggests that the higher the stiffness of the graft, the greater the level of fibrosis in the graft.

Migration and adipogenesis of ASCs

Immunofluorescence staining revealed that more CD34-positive cells were present in the 0.10 g/ml group than in the 0.05 and 0.075 g/ml groups on days 7, 14 and 30. However, the 0.075 g/ml group appeared to contain more perilipin-positive areas than the 0.05 and 0.10 g/ml groups on days 7, 14 and 30 (Figure 5a). A quantitative analysis

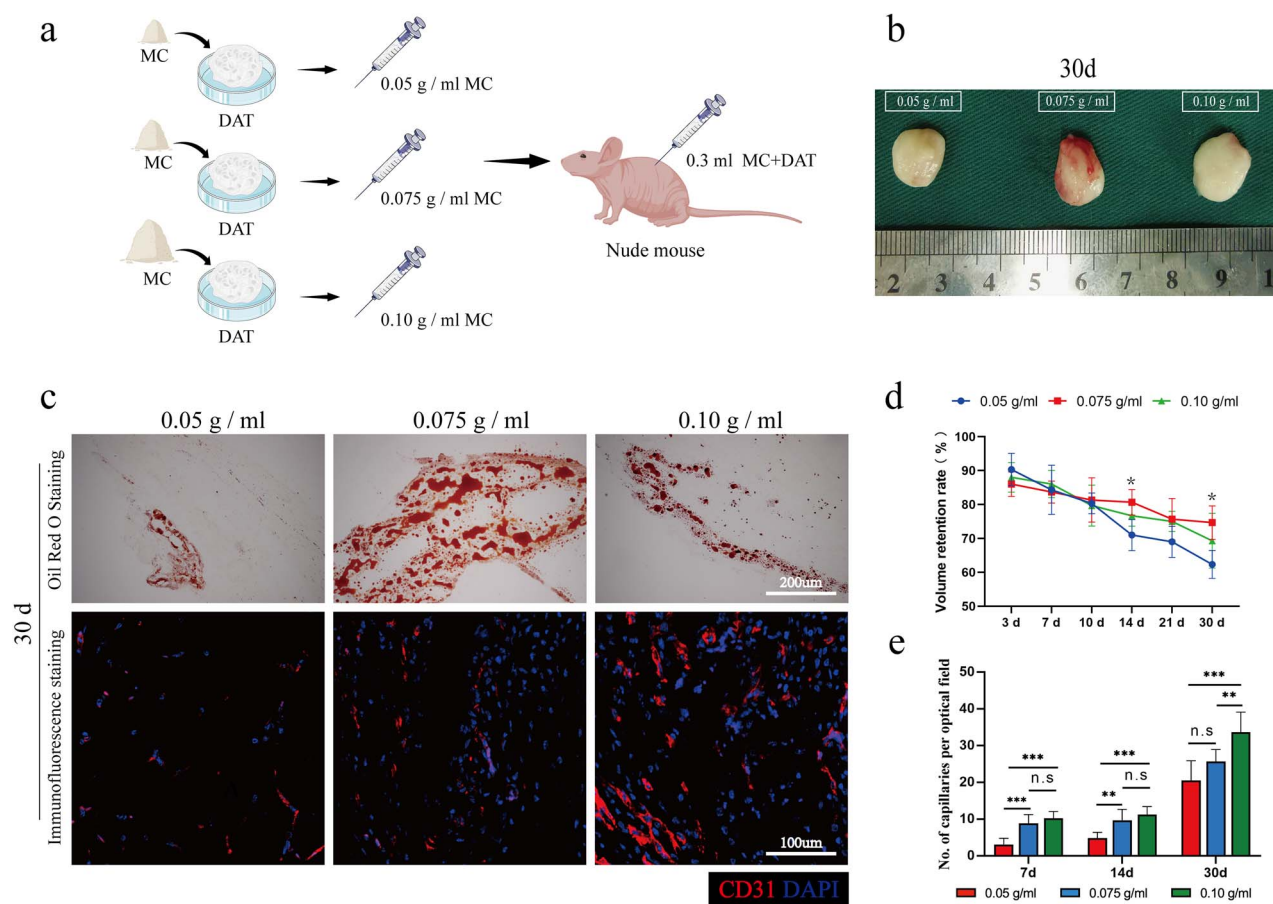


Figure 3. Sample volume, oil red O staining and vascularization of grafts. (a) Schematic illustration of the setup of the animal experiment. (b) Gross morphology of grafts in the three groups on day 30 after injection into nude mice. (c) Oil red O staining of grafts in the three groups on day 30. Immunofluorescence staining of CD31 (red) and DAPI (blue) in the three groups on day 30. (d) Percentage volume retention of the grafts in each group on days 3, 7, 10, 14, 21 and 30 (* $p < 0.05$). (e) Quantification of CD31-positive areas (number of capillaries per optical field) in grafts in the three groups on days 7, 14 and 30 (** $p < 0.01$, *** $p < 0.001$, *n.s.*, no significance; $n = 7$). Scale bar: 200 or 100 μm . DAT decellularized adipose tissue, MC methyl cellulose, DAPI 4',6-diamidino-2-phenylindole

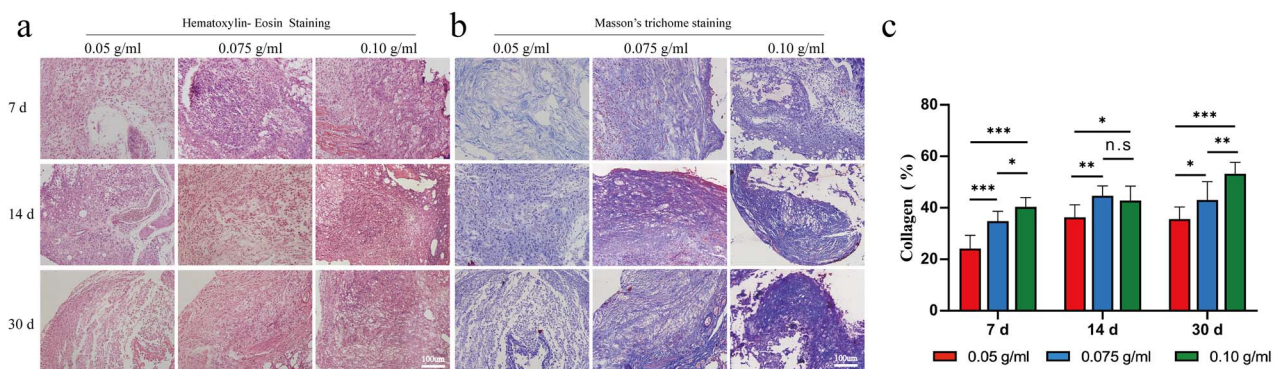


Figure 4. Histological analysis of grafts in the three groups on days 7, 14 and 30. (a) Hematoxylin–eosin staining of grafts. (b) Masson's trichrome staining of grafts. (c) The percentage of collagen in grafts (* $p < 0.05$, ** $p < 0.01$, *** $p < 0.001$, *n.s.*, no significance; $n = 7$). Scale bar: 100 μm

of the stained samples confirmed these visual observations. Specifically, on days 7, 14 and 30, the 0.05 g/ml group had fewer CD34-positive cells than the 0.075 g/ml group ($p < 0.01$ or $p < 0.001$) and 0.10 g/ml group ($p < 0.001$), and the 0.075 g/ml group had fewer CD34-positive cells than the 0.10 g/ml group ($p < 0.05$ or $p < 0.01$) (Figure 5b). On days 7, 14 and 30, the number of perilipin-positive cells in the

0.075 g/ml group was significantly higher than that in the 0.05 g/ml group ($p < 0.01$ or $p < 0.001$) and 0.10 g/ml group ($p < 0.05$ or $p < 0.001$) (Figure 5c). The number of perilipin-positive cells in the 0.10 g/ml group was significantly higher than that in the 0.05 g/ml group ($p < 0.05$) on day 14 only (Figure 5c). This indicates that as graft stiffness increases, the number of ASCs migrating into the graft increases, but

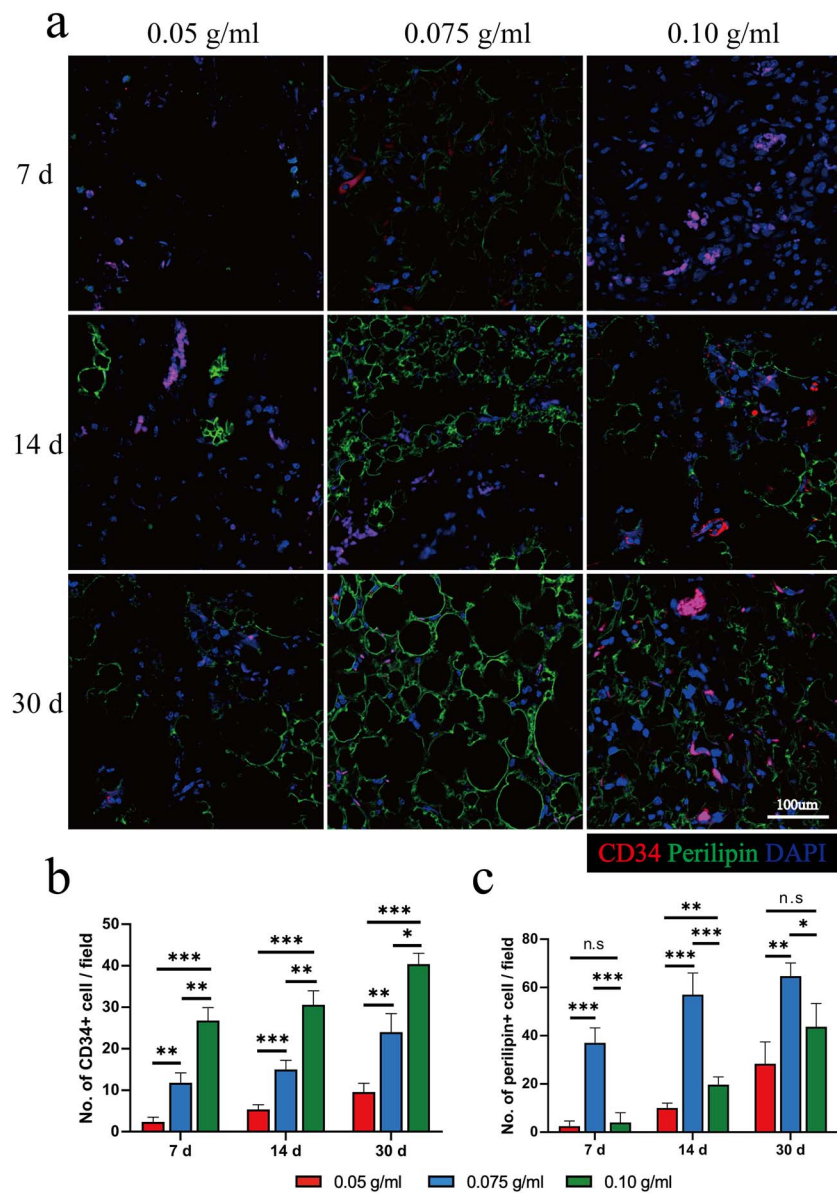


Figure 5. Migration and adipogenesis of adipose-derived stem cells. (a) Immunofluorescence staining of CD34 (red), perilipin (green) and DAPI (blue) in the three groups on days 7, 14 and 30. (b) Quantification of CD34-positive cells in grafts from the three groups on days 7, 14 and 30. (c) Quantification of perilipin-positive cells in grafts from the three groups on days 7, 14, and 30 (* $p < 0.05$, ** $p < 0.01$, *** $p < 0.001$, *n.s.*, no significance; $n = 7$). Scale bar = 100 μm . DAPI 4',6-diamidino-2-phenylindole

adipogenic differentiation of ASCs is inhibited if stiffness is too high.

Expression of adipogenesis-associated proteins

Western blotting was used to examine the expression levels of PPAR- γ , C/EBP and aP2 in the three groups on days 14 and 30 (Figure 6a). Compared with that in the 0.10 g/ml group, PPAR- γ expression was higher in the 0.05 g/ml group ($p < 0.05$) and 0.075 g/ml group ($p < 0.05$) on day 14 (Figure 6b). In addition, PPAR- γ expression in the 0.075 g/ml group was higher than that in the 0.05 g/ml group ($p < 0.01$) and 0.10 g/ml group ($p < 0.05$) on day 30 (Figure 6b). aP2 expression was higher in the 0.075 g/ml group ($p < 0.05$) and 0.10 g/ml group ($p < 0.01$) than in the 0.05 g/ml group on

day 14, and was higher in the 0.075 g/ml group than in the 0.05 g/ml group ($p < 0.01$) and 0.10 g/ml group ($p < 0.01$) on day 30 (Figure 6c). C/EBP α expression was higher in the 0.075 g/ml group than in the 0.05 and 0.10 g/ml groups on days 14 and day 30 (all $p < 0.05$) (Figure 6d).

Discussion

In this study, we physically cross-linked three different concentrations of MC with an equal volume of DAT to generate cell-free hydrogel systems with varying degrees of stiffness. Increasing the stiffness of the cell-free hydrogel system promoted the migration of ASCs and vascularization after grafting. Adipogenesis of ASCs and adipose regeneration

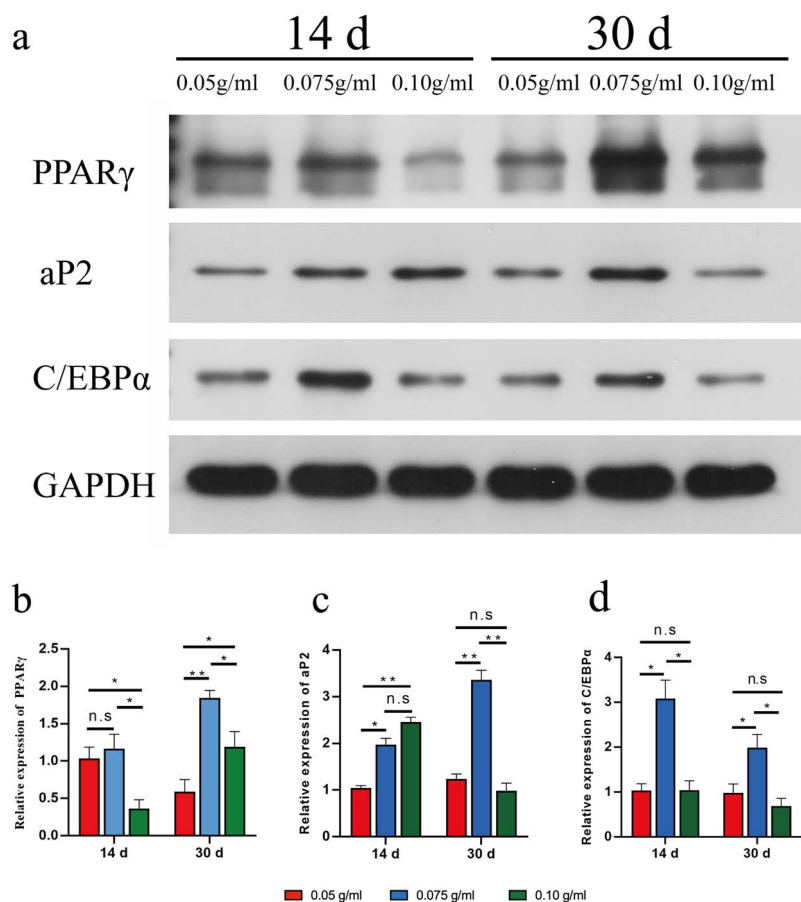


Figure 6. Western blot analyses of adipogenesis-associated proteins. (a) Expression levels of PPAR- γ , aP2 and C/EBP α in grafts from the three groups on days 14 and 30. (b-d) Quantification of the PPAR- γ , aP2 and C/EBP α band intensities, respectively, in the three groups on days 14 and 30; * $p < 0.05$, ** $p < 0.01$; $n = 7$. PPAR- γ peroxisome proliferator-activated receptor gamma, C/EBP α transcription factor CCAAT/enhancer-binding protein alpha, aP2 adipocyte protein 2, GAPDH glyceraldehyde-3-phosphate dehydrogenase, n.s. no significance

were highest in the system generated using MC at a concentration of 0.075 g/ml (Figure 7). Compared with the grafting of DAT that we performed previously (Figure S1), vascularization and adipogenesis of DAT were significantly improved in the 0.075 g/ml group.

The use of human tissue can reduce concerns related to immune responses/sensitization and transmission of heterologous diseases, which are often associated with animal products such as bovine and porcine collagen. Adipose tissue is an abundant and accessible source of human stem cells and ECM and is therefore useful for tissue-engineering applications [15,16,18,20–22]. However, the antigenic components of cells in adipose tissue limit their use in homologous allografts. The decellularization protocol developed in our current study, which uses DAT prepared by collecting large volumes of intact ECM containing basement membrane components, promises to be a valuable development in tissue engineering [23,24]. Numerous studies have attempted to use DAT as a biological scaffold to treat different types of tissue defects, such as skin, cartilage and bone defects, with initial success [6,24–28]. In particular, remarkable achievements have been made in repairing soft tissue volume deficiencies and defects

by inducing adipose regeneration. A pre-clinical and clinical study reported promising fat regeneration when DAT was injected into mice and the wrists of humans, suggesting that subcutaneously implanted DAT with retained angiogenic and adipogenic factors could serve as an inducible scaffold to sustain adipogenesis and has potential for clinical applications [12]. However, the ability of ordinary DAT to support adipogenic differentiation of ASCs is hindered by its excessive stiffness. In recent years, numerous studies have attempted to modulate the stiffness or morphology of DAT using a variety of chemical approaches to facilitate lipogenic differentiation [24]. Kim *et al.* used poly (l-lactide-co-caprolactone) scaffolds combined with DAT and ASCs to successfully prepare scaffolds that can promote adipogenesis and angiogenesis [29]. By combining bioresorbable polycaprolactone and DAT, Zhang *et al.* fabricated porous bioscaffolds that successfully induced the formation of highly vascularized adipose tissue in a rabbit model [30]. However, such chemical approaches have negative effects on adipose regeneration due to excessive destruction of biologically loaded factors in DAT or residual chemical cross-linking agents. To overcome these problems, there is an urgent need to explore safer and more

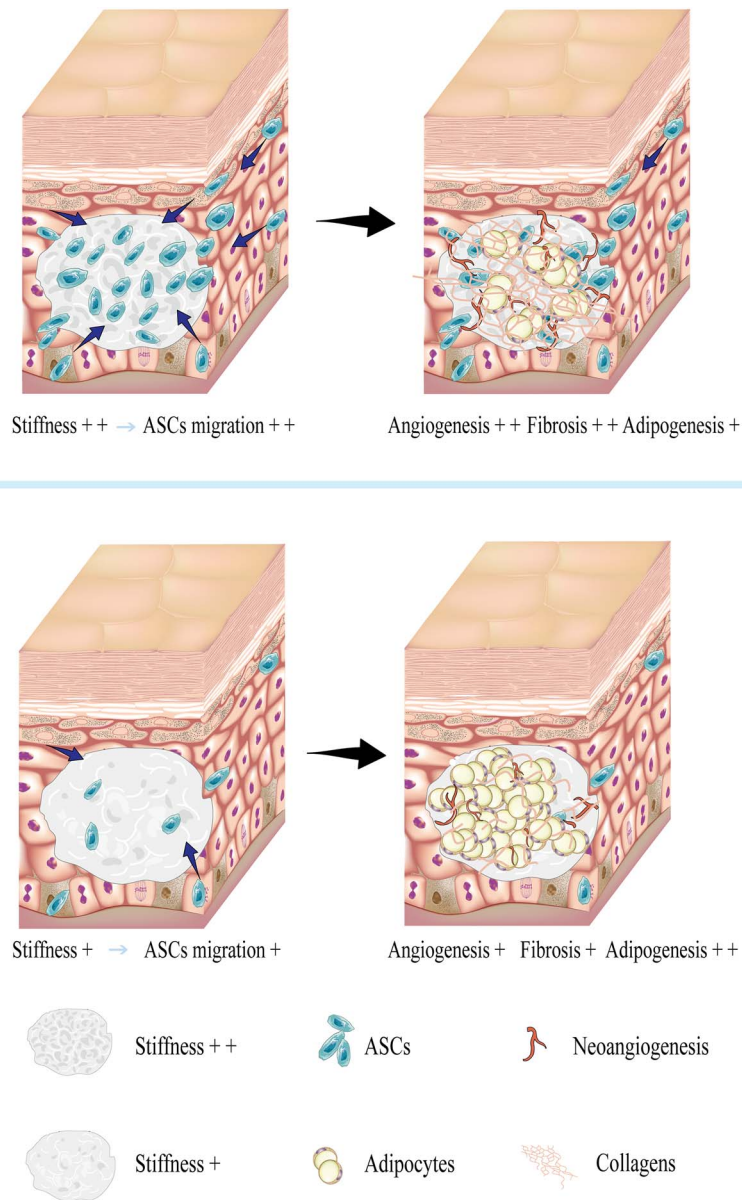


Figure 7. Overview of the potential mechanism by which changes in cell-free hydrogel system stiffness promote adipose regeneration by regulating angiogenesis, ASC migration and adipogenesis. + increase, ++ dramatic increase. ASCs adipose-derived stem cells

convenient physical ways to regulate the hardness of DAT. MC is a nonionic cellulose ether that is made by introducing methyl groups into cellulose through etherification [31]. MC is approved by the food and drug administration (FDA) as a thickening agent for water-soluble adhesives. Due to its low biotoxicity and stable physicochemical properties, MC is widely used for clinical purposes [32–34] and to adjust the gel properties of drugs and other materials [35,36]. MC rapidly degrades when transplanted alone *in vivo* and this feature makes it suitable for adjusting the stiffness of DAT. The cell-free hydrogel system described here was mainly composed of collagen and did not contain cellular components, thereby maintaining the original components of DAT, which could serve as a scaffold for tissue-engineering applications while also providing sufficient space for seed cells to regenerate

[37,38]. Based on the ability of the cell-free hydrogel system to promote the migration and lipogenic differentiation of ASCs demonstrated in this study, we believe that this system has the potential to repair soft tissue defects caused by tumors and trauma in clinical settings by promoting adipose regeneration.

ASCs are used as seed cells for adipose regeneration in tissue-engineering applications [39–41] and their function can be regulated by the stiffness of scaffolds [14]. Cell migration, which is central to many biological processes, including wound healing, tissue regeneration and cancer progression, is sensitive to environmental stiffness [42]. Allieux-Guérin *et al.* found that stiffness gradients control cell contraction by regulating myosin, and that cells migrate at a constant rate toward areas of high stiffness [43]. In addition, Young *et al.*

reported that ASCs are more sensitive to stiffness than mesenchymal stem cells when cultured on polyacrylamide gels [44]. In our current study, we found that increasing the stiffness of the cell-free hydrogel system promoted the migration of ASCs.

We also found that increasing the stiffness of the cell-free hydrogel system promoted vascularization after grafting. Indeed, angiogenesis and network formation are regulated by stiffness [45,46]. Early-stage angiogenesis in adipose tissue is very important for regeneration after grafting [47,48]. However, fine vascularization and sufficient supply of seed cells did not lead to better adipose regeneration in our current study. Furthermore, adipose regeneration was only promoted in the cell-free hydrogel system made with MC at a concentration of 0.075 g/ml. These findings might be related to the effect of stiffness on the differentiation of ASCs [14,35]. Although the *in vivo* stiffness of a cell-free hydrogel system is highly dynamic due to biological processes such as cell infiltration and ECM degradation, it is clear that the stiffness property influences the differentiation of ASCs. In previous studies, a variety of hydrogel systems were used to investigate the relationship between cellular behaviors and the elasticity of native tissues, including brain (~0.2–1 kPa), adipose (2–4 kPa) and muscle (~10 kPa), as well as osteoids (~30–45 kPa) [49–52].

Sequential expression of PPAR- γ , C/EBP and aP2 plays an important role in the terminal differentiation of preadipocytes into triglyceride-laden adipocytes [53]. The expression levels of these three proteins were significantly higher in the 0.075 g/ml group than in the 0.05 or 0.10 g/ml groups on days 14 and 30. These findings suggest that the cell-free hydrogel system generated using MC at a concentration of 0.075 g/ml formed a soft gel with favorable stiffness (~4 kPa) to promote the adipogenic differentiation of stem cells. Therefore, the adipogenesis of ASCs and adipose regeneration were highest in the cell-free hydrogel system with MC at 0.075 g/ml.

Conclusion

Adjusting the stiffness of DAT using the MC method described in this study can effectively promote adipose regeneration, which is of great significance to the development of methods for the effective repair and reconstruction of large-volume soft tissue defects. Next, although there remains a gap between animal models and actual clinical applications, we will try to apply this cell-free hydrogel system to the clinical setting. In the future, the ability of this cell-free hydrogel system to regenerate adipose tissue may be further enhanced by optimizing the preparation process, such as pre-loading cells or growth factors, thus making it more convenient, safe and effective for clinical applications.

Abbreviations

aP2: Anti-adipocyte protein 2; ASC: Adipose-derived stem cell; BCA: bicinchoninic acid; C/EBP α : CCAAT/

enhancer-binding protein alpha; DAT: Decellularized adipose tissue; DAPI: 4',6-diamidino-2-phenylindole; ECM: Extracellular matrix; FDA: U.S. Food and Drug Administration; GAPDH: glyceraldehyde-3-phosphate dehydrogenase; MC: Methyl cellulose; PPAR γ : Peroxisome proliferator-activated receptor gamma.

Supplementary data

Supplementary data is available at *Burns & Trauma Journal* online.

Funding

This work was supported by the following organizations: National Nature Science Foundation of China (81601702, 81671931, 81772101, 81701920, 81801933, 81801932, 81871573, 81901976, 81901975, 81971852, 8207081184, 82002052); Natural Science Foundation of Guangdong Province of China (2021A1515011623); Medical Scientific Research Foundation of Guangdong Province of China (A2020542); Science and Technology Program of Guangzhou of China (201604020007); Fundamental and applied fundamental Research Regional United Fund of Guangdong Province (2019A1515110112); Administrator Foundation of Nanfang Hospital (2019B021, 2020Z004); and the National Undergraduate Innovation and Entrepreneurship Training Program (X202012121222, X202012121312).

Authors' contributions

YL, XB and MFW designed the experiments and wrote the manuscript. YL, XB and XYC performed the experiments. YL and WQZ analyzed the data. XB performed the statistical analysis and revised the manuscript. MFW, XYC and WQZ contributed reagents, materials and analysis tools. ZQD and FL provided equipment and research funds and approved the final submission. All authors read and approved the final manuscript.

Ethics approval and consent to participate

All animal procedures were approved under the guidelines of Animal Ethics Committee of Southern Medical University, Nanfang Hospital (Guangzhou, China) (approval number NFYY-2020-0581).

Conflicts of interest

The authors declare that they have no conflicts of interest.

Data availability statement

The data underlying this article will be shared on reasonable request to the corresponding author.

References

- Wei FC, Celik N, Chen HC, Cheng MH, Huang WC. Combined anterolateral thigh flap and vascularized fibula osteoseptocutaneous flap in reconstruction of extensive composite mandibular defects. *Plast Reconstr Surg.* 2002;109:45–52.
- Kamat P, Frueh FS, McLuckie M, Sanchez-Macedo N, Wolint P, Lindenblatt N, et al. Adipose tissue and the vascularization of biomaterials: stem cells, microvascular fragments and nanofat-a review. *Cytotherapy.* 2020;22:400–11.
- Li X, Cho B, Martin R, Seu M, Zhang C, Zhou Z, et al. Nanofiber-hydrogel composite-mediated angiogenesis for soft tissue reconstruction. *Sci Transl Med.* 2019;11:eaau6210.
- Lucas JB. The physiology and biomechanics of skin flaps. *Facial plastic surgery clinics.* 2017;25:303–11.
- Clauser L, Zavan B, Galiè M, Di Vittorio L, Gardin C, Bianchi AE. Autologous fat transfer for facial augmentation: surgery and regeneration. *J Craniofac Surg.* 2019;30:682–5.
- Mohiuddin OA, Campbell B, Poche JN, Thomas-Porch C, Hayes DA, Bunnell BA, et al. Decellularized adipose tissue: biochemical composition, in vivo analysis and potential clinical applications. *Adv Exp Med Biol.* 2020;1212:57–70.
- Xia Z, Guo X, Yu N, Zeng A, Si L, Long F, et al. The application of Decellularized adipose tissue promotes wound healing. *Tissue Eng Regen Med.* 2020;17:863–74.
- Dong J, Yu M, Zhang Y, Yin Y, Tian W. Recent developments and clinical potential on decellularized adipose tissue. *J Biomed Mater Res A.* 2018;106:2563–74. <https://doi.org/10.1002/jbm.a.36435>.
- Morissette Martin P, Shridhar A, Yu C, Brown C, Flynn LE. Decellularized adipose tissue scaffolds for soft tissue regeneration and adipose-derived stem/stromal cell delivery. *Methods in Molecular Biology (Clifton, NJ).* 2018;1773:53–71. https://doi.org/10.1007/978-1-4939-7799-4_6.
- Porzionato A, Stocco E, Barbon S, Grandi F, Macchi V, De Caro R. Tissue-engineered grafts from human Decellularized extracellular matrices: a systematic review and future perspectives. *Int J Mol Sci.* 2018;19:4117.
- Flynn LE. The use of decellularized adipose tissue to provide an inductive microenvironment for the adipogenic differentiation of human adipose-derived stem cells. *Biomaterials.* 2010;31:4715–24.
- Kokai LE, Schilling BK, Chnari E, Huang YC, Imming EA, Karunamurthy A, et al. Injectable allograft adipose matrix supports Adipogenic tissue Remodeling in the nude mouse and human. *Plast Reconstr Surg.* 2019;143:299e–309. <https://doi.org/10.1097/PRS.0000000000005269>.
- Zhang Z, Qu R, Fan T, Ouyang J, Lu F, Dai J. Stepwise Adipogenesis of Decellularized cellular extracellular matrix regulates adipose tissue-derived stem cell migration and differentiation. *Stem Cells Int.* 2019;2019:1–11. <https://doi.org/10.1155/2019/1845926>.
- Li Y, Wu M, Zhang Z, Xia J, Wang Z, Chen X, et al. Application of external force regulates the migration and differentiation of adipose-derived stem/pro genitor cells by altering tissue stiffness. *Tissue Eng Part A.* 2019;25:1614–22.
- Tanzi MC, Farè S. Adipose tissue engineering: state of the art, recent advances and innovative approaches. *Expert Rev Med Devices.* 2009;6:533–51.
- Gomillion CT, Burg KJ. Stem cells and adipose tissue engineering. *Biomaterials.* 2006;27:6052–63.
- Ramírez-Zacarias JL, Castro-Muñozledo F, Kuri-Harcuch W. Quantitation of adipose conversion and triglycerides by staining intracytoplasmic lipids with oil red O. *Histochemistry.* 1992;97:493–7.
- Beeson W, Woods E, Agha R. Tissue engineering, regenerative medicine, and rejuvenation in 2010: the role of adipose-derived stem cells. *Facial Plast Surg.* 2011;27:378–88.
- Cai J, Feng J, Liu K, Zhou S, Lu F. Early macrophage infiltration improves fat graft survival by inducing angiogenesis and hematopoietic stem cell recruitment. *Plast Reconstr Surg.* 2018;141:376–86. <https://doi.org/10.1097/PRS.00000000000004028>.
- He Y, Lin M, Wang X, Guan J, Dong Z, Lu F, et al. Optimized adipose tissue engineering strategy based on a neo-mechanical processing method. *Wound Repair Regen.* 2018;26:163–71. <https://doi.org/10.1111/wrr.12640>.
- Choi JS, Yang HJ, Kim BS, Kim JD, Kim JY, Yoo B, et al. Human extracellular matrix (ECM) powders for injectable cell delivery and adipose tissue engineering. *J Control Release.* 2009;139:2–7.
- Tan QW, Zhang Y, Luo JC, Zhang D, Xiong BJ, Yang JQ, et al. Hydrogel derived from decellularized porcine adipose tissue as a promising biomaterial for soft tissue augmentation. *J Biomed Mater Res A.* 2017;105:1756–64.
- Choudhury D, Yee M, Sheng ZLJ, Amirul A, Naing MW. Decellularization systems and devices: state-of-the-art. *Acta Biomater.* 2020;115:51–9.
- Yang JZ, Qiu LH, Xiong SH, Dang JL, Rong XK, Hou MM, et al. Decellularized adipose matrix provides an inductive microenvironment for stem cells in tissue regeneration. *World J Stem Cells.* 2020;12:585–603.
- Ahn WB, Lee YB, Ji YH, Moon KS, Jang HS, Kang SW. Decellularized human adipose tissue as an alternative graft material for bone regeneration. *Tissue Eng Regen Med.* 2022;19:1089–98.
- Kesim MG, Durucan C, Atila D, Keskin D, Tezcaner A. Decellularized adipose tissue matrix-coated and simvastatin-loaded hydroxyapatite microspheres for bone regeneration. *Biotechnol Bioeng.* 2022;119:2574–89.
- Adem S, Abbas DB, Lavin CV, Fahy EJ, Griffin M, Diaz Deleon NM, et al. Decellularized adipose matrices can alleviate radiation-induced skin fibrosis. *Adv Wound Care.* 2022;11:524–36.
- Ibsirlioglu T, Elçin A, Elçin Y. Decellularized biological scaffold and stem cells from autologous human adipose tissue for cartilage tissue engineering. *Methods.* 2020;171:97–107.
- Kim SH, Kim D, Cha M, Kim SH, Jung Y. The regeneration of large-sized and vascularized adipose tissue using a tailored elastic scaffold and dECM hydrogels. *Int J Mol Sci.* 2021;22:12560. <https://doi.org/10.3390/ijms22212560>.
- Zhang G, Ci H, Ma C, Li Z, Jiang W, Chen L, et al. Additively manufactured macroporous chambers facilitate large volume soft tissue regeneration from adipose-derived extracellular matrix. *Acta Biomater.* 2022;148:90–105.
- Kim MH, Park H, Nam HC, Park SR, Jung JY, Park WH. Injectable methylcellulose hydrogel containing silver oxide nanoparticles for burn wound healing. *Carbohydr Polym.* 2018;181:579–86.
- Tudbury PB. Clinical trial of a methyl cellulose solution. *J Am Med Womens Assoc.* 1952;7:126–8.

33. Coetzee N, Blanchard K, Ellertson C, Hoosen AA, Friedland B. Acceptability and feasibility of Micralax applicators and of methyl cellulose gel placebo for large-scale clinical trials of vaginal microbicides. *AIDS*. 2001;15:1837–42.
34. Mostafaei A, Taheri N, Ghojzadeh M, Latifi A, Moghadam N. Comparison of the effect of mitomycin C and bevacizumab-methylcellulose mixture on combined phacoemulsification and non-penetrating deep sclerectomy surgery on the intraocular pressure (a clinical trial study). *Int Ophthalmol*. 2019;39:2341–51.
35. Campiglio CE, Villonio M, Dellacà RL, Mosca F, Draghi L. An injectable, degradable hydrogel plug for tracheal occlusion in congenital diaphragmatic hernia (CDH). *Mater Sci Eng C Mater Biol Appl*. 2019;99:430–9.
36. Jamard M, Hoare T, Sheardown H. Nanogels of methylcellulose hydrophobized with N-tert-butylacrylamide for ocular drug delivery. *Drug Deliv Transl Res*. 2016;6:648–59.
37. Ren Y, Zhang Y, Zhang H, Wang Y, Liu L, Zhang Q. A Gelatin-hyaluronic acid double cross-linked hydrogel for regulating the growth and dual dimensional cartilage differentiation of bone marrow mesenchymal stem cells. *J Biomed Nanotechnol*. 2021;17:1044–57.
38. Stowers RS. Advances in extracellular matrix-mimetic hydrogels to guide stem cell fate. *Cells Tissues Organs*. 2021;211:703–20.
39. Yang J, Zhou C, Fu J, Yang Q, He T, Tan Q, et al. In situ Adipogenesis in biomaterials without cell seeds: current status and perspectives. *Front Cell Dev Biol*. 2021;9:647149.
40. Minter D, Marra KG, Rubin JP. Adipose-derived mesenchymal stem cells: biology and potential applications. *Adv Biochem Eng Biotechnol*. 2013;129:59–71.
41. Leslie SK, Cohen DJ, Hyzy SL, Dosier CR, Nicolini A, Sedlaczek J, et al. Microencapsulated rabbit adipose stem cells initiate tissue regeneration in a rabbit ear defect model. *J Tissue Eng Regen Med*. 2018;12:1742–53.
42. Bangasser BL, Shamsan GA, Chan CE, Opoku KN, Tüzel E, Schlichtmann BW, et al. Shifting the optimal stiffness for cell migration. *Nat Commun*. 2017;8:15313. <https://doi.org/10.1038/ncomms15313>.
43. Allieux-Guerin M, Icard-Arcizet D, Durieux C, Hénon S, Gallet F, Mevel JC, et al. Spatiotemporal analysis of cell response to a rigidity gradient: a quantitative study using multiple optical tweezers. *Biophys J*. 2009;96:238–47. <https://doi.org/10.1529/biophysj.108.134627>.
44. Young DA, Choi YS, Engler AJ, Christman KL. Stimulation of adipogenesis of adult adipose-derived stem cells using substrates that mimic the stiffness of adipose tissue. *Biomaterials*. 2013;34:8581–8.
45. Bao M, Chen Y, Liu JT, Bao H, Wang WB, Qi YX, et al. Extracellular matrix stiffness controls VEGF165 secretion and neuroblastoma angiogenesis via the YAP/RUNX2/SRSF1 axis. *Angiogenesis*. 2022;25:71–86.
46. Wang Y, Zhang X, Wang W, Xing X, Wu S, Dong Y, et al. Integrin $\alpha V\beta 5$ /Akt/Sp1 pathway participates in matrix stiffness-mediated effects on VEGFR2 upregulation in vascular endothelial cells. *Am J Cancer Res*. 2020;10:2635–48.
47. Yuan YI, Gao J, Lu F. Effect of exogenous adipose-derived stem cells in the early stages following free fat transplantation. *Exp Ther Med*. 2015;10:1052–8.
48. Nishimura T, Hashimoto H, Nakanishi I, Furukawa M. Microvascular angiogenesis and apoptosis in the survival of free fat grafts. *Laryngoscope*. 2000;110:1333–8.
49. Wei Z, Zhao J, Chen YM, Zhang P, Zhang Q. Self-healing polysaccharide-based hydrogels as injectable carriers for neural stem cells. *Sci Rep*. 2016;6:37841.
50. Kim JS, Choi JS, Cho YW. Cell-free hydrogel system based on a tissue-specific extracellular matrix for in situ adipose tissue regeneration. *ACS Appl Mater Interfaces*. 2017;9:8581–8. <https://doi.org/10.1021/acsami.6b16783>.
51. Floren M, Bonani W, Dharmarajan A, Motta A, Migliaresi C, Tan W. Human mesenchymal stem cells cultured on silk hydrogels with variable stiffness and growth factor differentiate into mature smooth muscle cell phenotype. *Acta Biomater*. 2016;31:156–66.
52. Wang X, Ding Z, Wang C, Chen X, Xu H, Lu Q, et al. Bioactive silk hydrogels with Tunable mechanical properties. *J Mater Chem B*. 2018;6:2739–46.
53. Prusty D, Park BH, Davis KE, Farmer SR. Activation of MEK/ERK signaling promotes adipogenesis by enhancing peroxisome proliferator-activated receptor gamma (PPARgamma) and C/EBPalpha gene expression during the differentiation of 3T3-L1 preadipocytes. *J Biol Chem*. 2002;277:46226–32.